Linear-Combination-of-Atomic-Orbitals Band Structure of TlBr†*

John Overton and John P. Hernandez
Physics Department, University of North Carolina, Chapel Hill, North Carolina 27514
(Received 18 May 1972)

Valence bands and rough estimates for conduction bands of TlBr are calculated using the linear-combination-of-atomic-orbitals approximation. The calculation is based on potentials and wave functions of the isolated ions obtained from solutions to the Dirac equation with a self-consistent Hartree–Slater potential. The crystal potential is constructed out of effective ionic potentials. In order to investigate the effects of correlation, two types of crystal potentials are constructed, one with the Slater exchange and the other with the Slater exchange modified to simulate the effects of correlation. These effects are found to be quantitatively important; however, the shapes and ordering of the bands are not affected. The band gap is found to be direct, at the X point of the simple-cubic Brillouin zone, and the three-lowest-energy optical-absorption peaks can be unambiguously assigned to transitions from the three-highest-energy-valence-band states at X to a common conduction band. Band masses are calculated at X. Expanding the lattice is found to cause an increase in the band gap. The results of the band-structure calculation allow a consistent interpretation of the experimental data.

I. INTRODUCTION

TlBr represents a class of materials with interesting properties about which, until recently, [1] few theoretical calculations have been made. This class of materials is intermediate between the extensively studied ionic alkali halides and the covalent semiconductors; in particular the thallium halides are highly polarizable, partly ionic, partly covalent insulators with a band gap of about 3 eV. Also, TlBr crystalizes in the CsCl structure with a lattice constant of 3.94 Å [2] at 0 K. The delay of theoretical work on these materials has been due to their more complicated nature as intermediate substances as well as due to the fact that thallium has a high atomic number ($Z = 81$) so that relativistic effects are important.

Theoretical interest in the thallium halides is partly a result of the large amount of experimental data that has become available. Measurements of their optical properties have been performed in absorption and reflection for bulk- and thin-film samples. [3–5] The temperature[3,5] and pressure[6,7] dependence of these measurements are also available and they show an effect intrinsic to the thallium halides. The first absorption peak shifts to higher energy as the temperature is increased or the pressure decreased[3,6,7] in contrast to the alkali halides which behave in the opposite manner. [8] Experimental results are also available for cyclotron resonance, [9] magnetoresistance, and the galvanomagnetic effects. [10]

This work is concerned with the knowledge that can be gained from the band structure and electronic states as they relate to the optical-absorption spectra, transport phenomena, and temperature and pressure effects on the first absorption peak of TlBr. The primary goal is to obtain an understanding of the states which give rise to the optical absorption[3] within a few electron volts of the band gap. In particular, this means assigning initial and final states as the source of the first few peaks. With the band structure and the knowledge of where the first transition occurs, the band masses are estimated for holes and electrons. The effect of pressure and temperature are partially examined by comparing band structures at lattice constants appropriate to 0 and 300 K. The resulting shifts of the bands should shed some light on the experimental behavior of the first absorption peak.

The results of this band-structure calculation are successful in that a consistent interpretation of the experimental data[3] is obtained. From the calculated band structure the band gap is found to be direct at the X point in the Brillouin zone and the initial and final states of the next two absorption peaks are also identified. The values of calculated band masses are in rough agreement with reported cyclotron-resonance experiments which also support the assignment of the band gap to the X point. [11] The calculated effect of changing the lattice parameter yields a reasonable explanation of temperature and pressure effects on the first optical-absorption peak.

The ionic nature of TlBr is exploited by using methods that were used in an ionic-alkali-halide calculation[12] and in the intermediate materials AgCl and AgBr. [13] [An augmented-plane-wave (APW) calculation[14] consistent with the AgCl and AgBr linear-combination-of-atomic-orbitals (LCAO) calculation is available for comparison.] That is, the LCAO method is used to calculate the band structure. In this method, as it is used for this work, a model crystal potential is constructed out of the potentials of free Tl and Br ions. The resulting model Hamiltonian is then diagonalized in

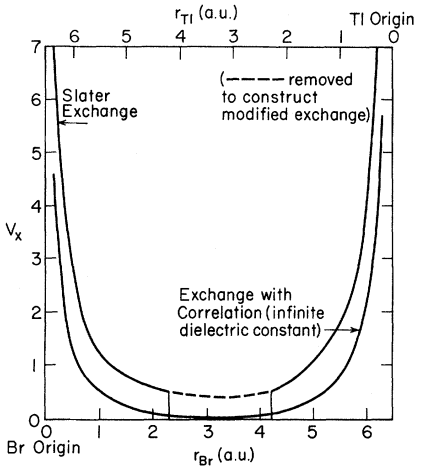

FIG. 1. Exchange potentials along the line joining a Br^- site and its nearest-neighbor Tl^+ site. The details for constructing the exchange with correlation may be found in Ref. 16.

a basis made up of the free Tl- and Br-ion states.

In addition to the success of the LCAO technique in the intermediate material AgBr there are several other reasons for choosing this method to calculate the band structure of TlBr. The calculational complication of the relativistic nature of Tl is avoided by using existing free-ion wave functions which are solutions to the Dirac equation with a self-consistent Hartree potential and a Slater exchange.[15] Further, the method is basically a first-principles calculation in that it would be the first step in a self-consistent calculation. Also, since electron states will be a linear combination of ionic states, interpretation of experimental data can be discussed from the free-ion viewpoint which is a help in visualizing the processes.

II. METHOD AND MODEL

The use of the LCAO method in this work consist of forming Bloch functions out of solutions of the Dirac equation for free Tl^+ and Br^- ions.[15] These ionic Bloch functions,

$$\psi_{kn}(\vec{r}) = (1/N^{1/2}) \sum_R e^{i\vec{k}\cdot\vec{R}}\, \psi_n(\vec{r} - \vec{R} - \vec{s}),$$

are used as a (nonorthogonal) basis set with which a model crystal Hamiltonian H is diagonalized. ψ_n is the nth free-ion state centered at $\vec{R}+\vec{s}$, where $\vec{R}$ is a lattice vector and $\vec{s}$ is a vector from the origin of the cell to the ion in question in that cell. Since these states $|k, n\rangle$ are not orthogonal, the eigenvalue problem is in the form

$$\Delta^{-1}(k)H(k)\; C_\alpha(k) = \epsilon_{\alpha k}\; C_\alpha(k),$$

where $\Delta(k)$ is the overlap matrix ($\langle jk|lk\rangle$); $H(k)$ is the Hamiltonian matrix in the ionic-Bloch-function basis ($\langle jk|H|lk\rangle$); and $C_\alpha(k)$ is the αth eigenvector whose elements specify the appropriate linear combination (of the ionic Bloch functions) that correspond to the αth eigenvalue $\epsilon_{\alpha k}$.

The model Hamiltonian was taken to be a kinetic energy term plus a sum of effective potentials from each of the ion sites in the crystal. The effective potential from each site consists of the nuclear-charge contribution, the direct Coulomb potential of the ion at the site (this is based on the assumption tion that the sum of the free-ion charge densities is a good approximation to the crystal charge density), and an effective-exchange contribution. The free-ion states were calculated self-consistently using a Slater exchange[15] (with an asymptotic correction, the Latter tail, which need not concern us here); thus a logical approximation to the crystal exchange is the Slater exchange $1.5[(3/\pi)\rho]^{1/3}$, where ρ is the sum of the free-ion charge densities at the point in question. This exchange ensures, in the regions near the ion sites where the ion wave functions associated with a given site are large, that the crystal exchange and the free-ion exchange are effectively the same. This near equality is crucial in a non-self-consistent calculation using a limited basis set . Since Robinson *et al.*[16] have pointed out that correlation effects would substantially decrease the exchange, especially in the small-charge-density regions (calculations on AgCl also corroborated this point[13]), band structures based on two different exchange potentials were calculated. The first uses a sum of effective-exchange potentials from each ion site which, in the sense of a least-squares fit, added up to the crystal Slater exchange. The second was obtained by reducing the first exchange in the low-charge-density regions—our somewhat arbitrary prescription, for this qualitative investigation, was to set the exchange potential to zero in the region where the sum of the free-ion charge densities was small (the prescription used is shown, along the line joining nearest neighbor Tl and Br ions, in Fig. 1). This second potential, the modified exchange, is a muffin-tin-type of exchange to qualitatively investigate the effects of correlation.

To complete the description of the method used a brief account of the Hamiltonian matrix elements given in the Appendix.

III. CALCULATIONAL RESULTS

A. Introduction

To gain some insight into the crystal problem, as well as to offer a point of reference, it is of interest to first discuss the free ionic states and to speculate on the effect of the crystal field on their energies by showing the Madelung shift. The ground-state solution for the free ions have, for Br^- and Tl^+, respectively, spherically symmetric configurations,

$(4s_{1/2})^2(4p_{1/2})^2(4p_{3/2})^4$ and $(5p_{1/2})^2(5p_{3/2})^4(5d_{3/2})^6(6s_{1/2})^2$ (only the relevant high-energy states are given). Tl^{+*} $6p$ excited states [configurations $\ldots(6s_{1/2})^1(6p_{1/2})^1$ and $\ldots(6s_{1/2})^1(6p_{3/2})^1$; there are no bound Br^{-*} excited states] were used to construct approximate conduction bands.

In Fig. 2 the highest free-ion energy levels have been schematically represented along with the relative energy levels that would result from the Madelung shift. Based on this diagram one can speculate that the most important ionic valence states will be the Tl^+ $6s$ and Br^- $4p$ states. States of lower energy are not expected to be very important. Since LCAO conduction bands constructed out of excited-ion states are usually poor, the inclusion of the Tl^{+*} $6p$ states in the basis set of states could possibly alter what would be otherwise good valence bands; a similar difficulty was found by the second set of authors in Ref. 1.

Preliminary calculations basically confirmed the above speculation: Ionic states needed in the basis for calculating the high-energy valence bands were the Tl^+ $6s$, Br^- $4p$, and the Br^- $4s$ states. Br^- $4s$ states were included because, unlike the Tl^+ $5d$ states, they do influence the lower-energy crystal valence states (derived from the Tl^+ $6s$ and Br^- $4p$ states). The excited Tl^+ states did adversely influence the valence bands and had to be omitted from the valence basis. However, pure Tl^{+*} $6p$ bands as very crude conduction bands were useful in that they reinforced the interpretation which will be proposed for the optical data, allowed estimates of electron

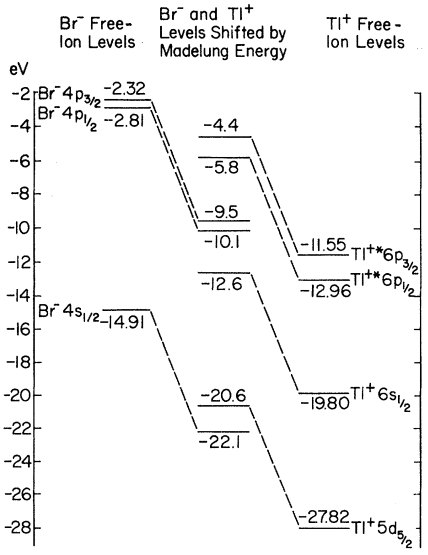

FIG. 2. Effect of the Madelung energy on the high-energy free-ion states. The ion states were calculated as in Ref. 15 and it should be noted that they are slightly high as compared to experiment: ~1 eV for Br^- and ~½ eV for Tl^+.

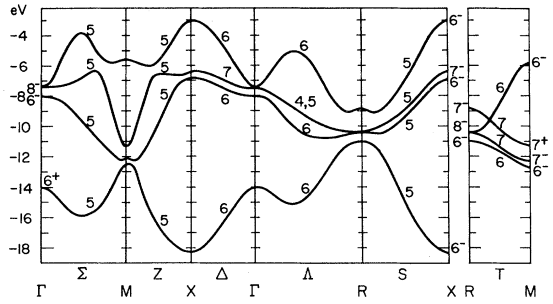

FIG. 3. Valence bands, Slater exchange, $T=0$ K.

masses, and helped in understanding the temperature and pressure effects on the first optical peak.

Four sets of valence bands were calculated. The bands were computed for each of the model Hamiltonians (Slater and modified-Slater exchanges) for lattice parameters corresponding to $T=0$ and 300 K. Also, conduction bands were approximated with the Tl^{+*} $6p$ states.

B. Energy Bands

Five ion states were needed in constructing the valence basis: Tl^+ $6s_{1/2,1/2}$, Br^- $4s_{1/2,1/2}$, Br^- $4p_{1/2,-1/2}$, Br^- $4p_{3/2,-1/2}$, and Br^- $4p_{3/2,3/2}$; the notation corresponds to n_{l_j,m_j}. Two sets of valence bands (for a 7.44-a.u.^{2} lattice parameter corresponding to $T=0$ K) have been calculated using the basis set. In all that follows the symmetry labels refer to a coordinate system with origin at a Br site. The first, Fig. 3, has been computed with the model Hamiltonian that has the Slater exchange, while the second, Fig. 4, is obtained using the modified Slater exchange. (The almost flat, basically Br^- $4s_{1/2}$, band which is lower in energy than any of the bands diagrammed is not shown; it is found at ~ −22 eV.)

As can be seen, both sets of bands have the same features with the contours of the corresponding bands in each set being essentially the same. The most important aspect of the two sets of bands is that the maximum energy is at the X point in the

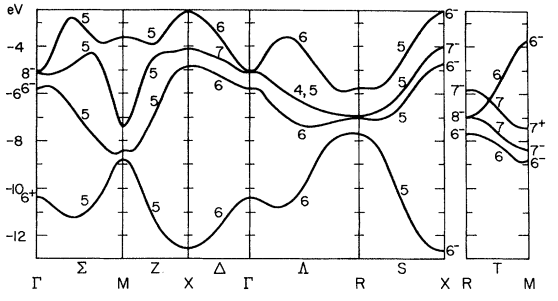

FIG. 4. Valence bands, modified exchange, $T=0$ K.

TABLE I. Selected matrix elements chosen to exhibit the effect of modifying the exchange.

		X Total[a]		Γ Total		R Total		M Total		On-site	
$\langle 1\,0\,\vert$	$\vert 2\,\vec{\xi}\rangle$	S[b]	MS[c]	S	MS	S	MS	S	MS	S	MS
$Tl^+ 6s_{1/2,1/2}$	$Tl^+ 6s_{1/2,1/2}$	6.2	11.0	3.8	10.0	8.8	11.3	7.8	11.3	6.8	11.0
$Tl^+ 6s_{1/2,1/2}$	$Br^- 4p_{3/2,3/2}$	$-i(6.6)$	$-i(2.8)$	0.0	0.0	0.0	0.0	0.0	0.0		
$Br^- 4p_{1/2,-1/2}$	$Br^- 4p_{1/2,-1/2}$	−8.0	−4.9	−4.5	−2.5	−8.5	−5.1	−8.5	−5.1	−7.9	−4.8
$Br^- 4p_{1/2,-1/2}$	$Br^- 4p_{3/2,-1/2}$	3.4	2.3	0.0	0.0	0.0	0.0	4.2	2.8	0.0	0.0

[a]The total matrix element is (see Appendix)

$$e^{i\vec{k}\cdot(\vec{s}_1-\vec{s}_2)}\left[\left(\sum_{\vec{\xi}\neq 0} e^{i\vec{k}\cdot\vec{\xi}}\langle 1\,0\left|H-\tfrac{1}{2}(E_1+E_2)\right|2\,\vec{\xi}\rangle\right)+\langle 1\,0\left|H-\tfrac{1}{2}(E_1+E_2)\right|2\,0\rangle\right];$$

the E_j's are free-ion energies; the last term is the on-site matrix element if $\vec{s}_1=\vec{s}_2$, and has no value if $\vec{s}_1\neq\vec{s}_2$.

[b]S is Slater exchange.

[c]MS is modified Slater exchange.

Brillouin zone. This and the next two lower energy states at X (whose separation energy is basically independent of the exchange) are most probably the initial states responsible, along with a common final state, for the three-lowest-energy optical transitions. The high-density-of-states regions in the Λ and Σ directions are also features unaltered by the exchange which will later be identified with optical phenomena.

There are, however, considerable quantitative differences in the two sets of bands. The modified-Slater-exchange results in narrower bands and reduced splittings between Tl^+- and Br^--derived bands bands. In fact, if the scale of the graph of the Slater set of bands, Fig. 3, was reduced by a factor of about $\frac{1}{3}$ and then rigidly shifted upward $\frac{1}{2}$ eV there would be little difference between the two sets of bands. For example, at the X point the top four bands span a range in energy which has been reduced from 15 to 10 eV, a reduction of $\frac{1}{3}$ by the exchange modification; while the splitting between the top state at X (Tl^+ and Br^- derived) and the next-lower state (Br^- derived) has been reduced by a factor of $\frac{1}{2}$ from 3.22 to 1.63 eV—a step in the right direction since, in our interpretation, the experimental splitting is 1 eV.

In order to obtain a better understanding of the two sets of band structures, matrix elements of the potential (so-called, for simplicity; they are defined below) will be discussed and related to these band structures.

Table I lists several matrix elements of the crystal potential with Slater exchange between ionic Bloch states at the high-symmetry points. (The corresponding potential matrix elements with modified exchange are also listed for comparison and will be discussed later.) From this table we can get an idea of the cumulative effect of the off-site matrix elements

$$\langle i0\left|H-\tfrac{1}{2}(E_i+E_j)\right|j\vec{\xi}\rangle,\ \vec{\xi}\neq 0;$$

$\vec{\xi}$ is the vector from the origin to an ion site, E_i is a free-ion energy. (That this is the relevant matrix element is shown in the Appendix.) For example, the on-site matrix element $\langle i0\,|\,H-E_i\,|\,i0\rangle$ for the potential (using the Slater exchange) is not far from the Madelung value of ±7.2 eV. However, at Γ the total matrix element for the Tl^+6s Bloch state is 3 eV lower than the on-site value of 6.8 eV. The difference between the total and the on-site value is due to the off-site matrix elements, indicating that the they are quite important. That is, some off-site contributions are 40% of the on-site, approximate Madelung, value.

The fact that the value of the on-site matrix element of the potential with the Slater exchange is near the Madelung value comes about because of the near equality of the crystal and ion potentials in most of the regions where wave-function amplitudes are non-negligible as well as from the fact that the overlaps are small.[17] Thus this matrix element is approximately that of the crystal field of all the ions except the origin ion.

When the exchange potential is modified, the matrix elements basically show two effects—the diagonal matrix elements increase and the nonzero off-diagonal matrix elements decrease in absolute magnitude. The first effect is easy to understand, since the exchange potential is binding, i.e, negative, setting it to zero in some region is equivalent to adding a positive potential and thus results in a diagonal-matrix-element increase. The decrease in magnitude of the off-diagonal matrix elements with the exchange modification does not have such an obvious explanation owing to possible cancellations between exchange and direct potentials and the effect may depend on the specific crystal structure of this problem.

After discussing the matrix elements it is possible to understand the behavior of the band structure as a result of modifying the exchange. The upward shift of the band is due basically to the in-

TABLE II. Effect of exchange on the top three energies (E) and wave functions at X.

		Expansion coefficients of the ionic Bloch states				
		E (eV)	$Tl^+ 6s_{1/2,+1/2}$	$Br^- 4p_{3/2,+3/2}$	$Br^- 4p_{3/2,-1/2}$	$Br^- 4p_{1/2,-1/2}$
1	S[a]	−3.08	$-i(0.98)$	+0.64	+0.37	−0.35
	M	−2.55	$-i(0.98)$	+0.66	+0.38	−0.27
2	S	−6.4	0.0	−0.56	+0.97	0.0
	M	−4.18	0.0	−0.56	+0.97	0.0
3	S	−6.94	$+i(0.10)$	+0.48	+0.28	+0.96
	M	−4.81	$+i(0.18)$	+0.44	+0.25	+0.98

[a]S is Slater exchange, M is modified exchange, $T=0$ K.

crease in energy as a result of increasing the exchange. The magnitude of the shift is probably an exaggeration that would not be as prominent if the free-ion states had been calculated with the modified exchange. That is, the on-site contributions are probably too large due to further emphasizing the difference between the free-ion and crystal potential. If the basis Bloch states were orthogonal, the splittings between the crystal states would be reduced by reducing the off-diagonal matrix elements. Even though the basis Bloch states are not orthogonal[17] it is reasonable to assume that the above is applicable; that is, splittings are determined primarily by off-diagonal matrix elements.

The effect on the crystal wave functions owing to modifying the exchange is not as noticeable as is the effect on the energies. This is partly due to symmetry. For example, at the R point the valence ionic Bloch states do not mix owing to symmetry, and thus the crystal wave functions, at this point, being composed of only one ionic Bloch state cannot be affected by the change in the exchange (or any potential with cubic symmetry). In regions such as the Σ direction, where all the Bloch functions mix, the expansion coefficients are altered by modifying the exchange; but the fractional changes in these coefficients are small when compared to the fractional change in the energies.

The effect of the exchange on the wave functions can be illustrated with the use of Table II. This table lists the expansion coefficients (of the ionic Bloch states) of the top three crystal valence states at the important X point. As can be seen, these wave functions are hardly changed as a result of the exchange modification.

In general, it is not possible to characterize a given band as either basically Tl^+ or basically Br^-. There is considerable interchange of the roles of states as one moves through the Brillouin zone. For example, the top band is pure $Br^- 4p_{3/2}$ at Γ, mixed with large components of Tl^+ and Br^- at X, and pure $Tl^+ 6s_{1/2}$ at R. The interchange of roles is a property of all the calculated bands except for the lowest energy band calculated (not shown in figures). This almost flat band is nearly pure $Br^- 4s_{1/2}$, a result not unexpected since the $Br^- 4s_{1/2}$ state was not expected (see Sec. III A and Fig. 2) to mix strongly with the higher states.

To aid in the interpretation of optical data, very crude approximations to conduction bands were made based on excited Tl^+ states (Tl^{+*} $6p$ states). The estimates resulted in a minimum energy state at X (6^+) and high-density-of-states regions along the Λ and Σ directions; these features were independent of the exchange approximation used. Though the estimates are not quantitatively helpful, the features mentioned above assist in interpreting the optical data (which will be discussed later).

C. Change in Lattice Parameter

Modification of the optical spectra caused by temperature or pressure changes is a result of the electron-phonon interaction. The effect of the phonons on the electrons can be divided into two, not uncoupled, aspect; one effect is through the rigid expansion of the lattice and the second is a dynamical interaction. The dynamical effects have been ignored since they are outside the scope of this work and the band structure has been calculated at a lattice parameter corresponding to 300 K (7.53 a.u. [2]). The resulting energies at X were compared to those calculated at the lattice parameter appropriate to 0 K. This comparison gives an estimate of the contribution due to lattice expansion to the energy shift of the first optical-absorption peak.

Table III lists the effects of lattice expansion on the top three valence states, at the high-symmetry points. As can be seen, there is a negative energy shift in the top valence energy at X with increasing lattice parameter. A plausible explanation as to why the top valence energy decreases can be found in the composition of this state. The state is dominated by $Tl^+ 6s$ (60% as measured by the squares of the expansion coefficients). As the crystal field is decreased by increasing the lattice parameter, pure ionic Tl^+ and Br^- states (in the crystal field) tend to decrease and increase in energy, respectively,

TABLE III. Changes in energy $[E_{300}-E_0\,(\mathrm{eV})]$ of the three-highest-energy valence-band states owing to lattice-parameter change.

	X		Γ		R		M	
	S[a]	M	S	M	S	M	S	M
1	−0.45	−0.29	+0.19	+0.16	−0.32	−0.29	+0.07	+0.05
2	+0.13	+0.09	+0.14	+0.08	+0.30	+0.20	−0.09	−0.15
3	+0.08	+0.03	0.0	+0.05	+0.31	+0.19	+0.34	+0.22

[a]S is Slater exchange, M is modified exchange.

owing to the decrease in the absolute value of the Madelung energy. Thus the two types of states are competing, when mixed, to lower or raise the energy of the state they comprise. Since the $Tl^+ 6s$ state dominates, it is reasonable to expect a negative energy shift in the top valence state at X. Further, the decrease in coupling should reduce the splitting between the first and third state (it can be seen in Fig. 3 that they are of the same symmetry) which also leads to a lowering of the highest state.

The negative energy shift is consistent with the positive energy shift of the first optical-absorption peak.[3,7] Of course knowledge of the energy shift of the lowest conduction band at X is highly desirable; however, these more diffuse states are most probably not affected as much by the lattice change as the valence states. (We found that the energy of the lowest Tl^{+*} $6p$ state at X increased slightly with T.) Hence, the direction of the shift of the valence state is responsible for the direction of the energy shift of the optical peak.

D. Band Masses

Since the constant-energy surfaces near X were found to be ellipsoids of revolution (a symmetry result) with axis of revolution along $\Delta(\Gamma \rightarrow X)$, longitudinal and transverse masses were calculated. Using the modified-exchange band structure, hole and electron masses were calculated with the following result; hole, $m^*/m = 0.35$ perpendicular to the axis of revolution and 0.60 along the axis. The electron-mass estimate gave $m^*/m = 0.26$ perpendicular to and 0.30 along the axis of revolution. With the Slater-exchange band structure, the masses are found to be as follows: hole, $m^*/m = 0.20$ and 0.36, respectively, perpendicular and parallel to the axis of revolution. The electron masses are essentially isotropic with $m^*/m = 0.25$.

IV. SUMMARY

Two sets of valence bands were calculated for the crystal with a lattice parameter corresponding to 0 K. The two sets of bands correspond to the two exchanges used. Both sets have the same important features: high point at X, next two lower states at X are basically split by the spin-orbit interaction of Br^-, and high density of states along the Λ and Σ directions. The highest state at X is about evenly divided between Tl^+ and Br^- components. The quantitative differences of the two sets of bands are more obvious than the qualitative differences. Bands calculated with the modified exchange are 30% narrower and the splittings between Tl^+- and Br^--derived bands are less than in the set of bands calculated with the Slater exchange. Wave functions are affected negligibly by the exchange modification.

The major features of the conduction bands approximated by using Tl^{+*} $6p$ states remain unaffected by the exchange modification; the low point is at X and there are high density of states in the Λ and Σ directions.

The effect on the first optical-absorption peak owing to increasing the lattice parameter was discussed. This shift was found to be positive in agreement with experiment and a plausible explanation for this positive shift was given.

Estimates for hole and electron masses at X were calculated. The surfaces of constant energy for the assumed lowest-energy electrons and holes in the crystal were found to be ellipsoids of revolution at X with the largest mass along the axis of revolution, the Δ direction (the electron mass is nearly isotropic).

V. DISCUSSION

Based on the calculated results, a discussion of the optical-absorption data follows. The three-lowest-energy optical-absorption peaks[3] are assigned to direct transitions from the three-highest valence states at X to a common conduction state. Since the experimental doublet (4.05 and 4.47 eV)[3] seems characteristic of the Br^- spin-orbit-split valence bands, the latter assignments seem natural. The calculated splitting between the first- and second- and the second- and the third-highest states at X are, respectively, 0.5 and 0.2 eV larger than they should be for quantitative agreement with experimental data. The observed shoulders (5.2 and 5.8 eV)[3] are most probably associated with the high-density-of-states regions in the Λ and Σ directions that occur in both the conduction

and valence bands. Assignments of the transitions at 5.0 and 6.1 eV [3] are more speculative. Direct transitions that could give rise to prominent optical peaks are $R_7^- \rightarrow R_7^+$, $R_7^- \rightarrow R_8^+$, and from the top-valence-band state to the second-conduction-band state at X. Other assignments are essentially transitions between the Br^- and Tl^+ sublattices (on the assumption that the conduction bands are basically Tl $6p$-like). For example, at R the states labeled R_7^-, R_8^-, and R_6^- are, respectively, pure Tl^+, pure Br^-, and pure Br^-, thus R_8^- (valence band) $\rightarrow R_7^+$ (conduction band) would be a Br^- to a Tl^+ sublattice transition. Since the overlaps are small, this type of transition is expected to be weak and thus they are excluded as possibilities.

The fundamental assumption behind the interpretation of the optical spectra is that the qualitative features of the calculated valence and crude conduction bands are essentially the same as those of the "real" band structure. This assumption seems reasonable especially in the case of the valence bands. The fundamental features of the bands were not altered nor was there much change in the expansion coefficients of the eigenstates (in contrast to the large quantitative change in the bands when the exchange was modified). Further, improving the exchange is expected to improve the band structure quantitatively by reducing splittings and narrowing bands. However, there is no reason to assume that the contours of the bands would change significantly—at least this is the expectation based on our experience with the rather severe change in the potential.

To end the discussion of the optical absorption, based on the results of this calculation, a speculation is offered to make plausible the experimental fact that the strength of the three-lowest-energy peaks are roughly the same. Our assignment of these peaks is to transitions from the three-highest-energy valence-band states at X to a common conduction band; yet the composition of the three initial states (from Table II) are, respectively, Tl^+ $6s$ and Br^- $4p$ components, pure Br^- $4p$, and mostly Br^- $4p$. If the conduction-band state were pure Tl^{+*} $6p$, then the second and third transitions would be very weak (in the Br to Tl sublattice transition, the overlaps are small[17]). So it seems reasonable to conclude that there is a non-negligible Br^- component to the lowest conduction-band state at X (for example, we found that Tl^{+*} $6p$ and Br^- $4s$ states, at X, did mix strongly).

There is a recent experiment[11] which is quite relevant to this work. Cyclotron-resonance measurements have been made on TlBr showing that the polaron-hole masses are anisotropic with a Δ-type or X symmetry. This experiment supports the calculated high-valence energy at X.

On the theoretical side there is a Korringa–Kohn–Rostoker (KKR) calculation of the band structure of TlBr and a Heine–Abarenkov model calculation of TlCl which are in general agreement with this work.[1] They obtain bands which are narrower and the splittings smaller than in this calculation. The major qualitative difference in the sets of bands is that in the KKR calculation the lowest conduction-band state at R is lower than that X; however, the authors state that their computed energy difference (lowest point at X to lowest at R: 0.3 eV) is within their error limits; thus they are prevented from a definitive ordering. This low energy R has led to the speculation (since the experimental electron masses are isotropic within the limits of the experimental accuracy) that the conduction-band minimum is at R where there is full cubic symmetry.[11] The Heine-Abarankov calculation obtains a conduction-band minimum at X in agreement with us. More work needs to be done to resolve the question about the low point of the conduction bands. Otherwise, all three theoretical calculations are in substantial agreement.

While quantitatively there is little doubt that a KKR-type calculation is more accurate than this work, the LCAO technique is quite helpful in complementing a more accurate method. The method in this work helps to visualize crystal states in terms of familiar ionic states, while a KKR technique has no such familiar point of reference.

Improvements within the framework of our technique can be made. This calculation is only qualitatively adequate in assigning energy values (to the states) for comparison with those experimentally obtained from optical transitions. A possible reason for this is that the free ionic states were calculated using a Slater–Latter exchange, whereas a more appropriate exchange for the crystal electrons is the exchange with correlation effects included as discussed previously. Figure 1 contrasts the crystal Slater exchange and an approximate crystal exchange that includes the crystal-correlation effects. The differences in the two exchanges are too large to treat in a limited basis calculation as in this work; so that a self-consistent potential and wave functions of free ions that reflect the correlation effects should be used. A model crystal potential and basis set constructed out of these new free-ion potentials and their wave functions should result in a better band structure. At least the experience of this work suggests that this would be the right direction to go for an improved LCAO calculation.

Another problem not considered in this work, or in the other existing calculations, is the possibility that there is significant charge redistribution owing to the computed strong mixing of the Tl^+ and Br^- Bloch wave functions. The charge density of the crystal differs from the sum of the free-ion charge

densities that were used to approximate the crystal potential, and thus a self-consistent calculation may be needed to resolve details such as the minimum-energy conduction-band state.

In summary, the LCAO calculation of the band structure of TlBr has led to a reasonable explanation of the optical spectra within a few electron volts of the band gap. A better understanding of the temperature and pressure effect on the first optical-absorption peak has been obtained. Anisotropic hole masses and essentially isotropic electron masses have been calculated, respectively, at the highest valence and lowest "conduction" states at X. Finally, one of the more important features to come out of this work is that one can obtain a large and useful amount of information about the energy bands and eigenstates in the intermediate materials using, *ab initio*, the LCAO technique.

ACKNOWLEDGMENTS

The authors wish to thank the Oak Ridge National Laboratory for kindly providing the wave functions and potentials used in this work (Ref. 15).

APPENDIX

The matrix elements of the Hamiltonian are needed in the ionic Bloch-function basis. Using translational symmetry, these matrix elements may be written as

$$\langle i\vec{k}|\,H\,|j\vec{k}\rangle = e^{i\vec{k}\cdot(\vec{s}_j-\vec{s}_i)}\sum_{\xi} e^{i\vec{k}\cdot\vec{\xi}}\,\langle i0|\,H\,|j\vec{\xi}\rangle, \qquad \text{(A1)}$$

where $\vec{\xi}$ is the vector from the origin of the ith function to the origin of the jth function. Typical matrix elements had to be summed to the sixth-neighbor shell.

Relativistic effects may essentially be taken into account by writing the Hamiltonian as

$$H=\tfrac{1}{2}(H^I_{i0}+H^I_{j\vec{\xi}})-\tfrac{1}{2}(V^I_{i0}+V^I_{j\vec{\xi}})+\varphi, \qquad \text{(A2)}$$

that is, adding and subtracting the free-ion potentials $V^I_{j\vec{\xi}}$ of the state in question; H^I_j is the free-ion Hamiltonian of the ion centered at $\vec{\xi}$ and φ is the crystal potential. Thus

$$\langle i0|\,H\,|j\vec{\xi}\rangle=\tfrac{1}{2}(E_i+E_j)\Delta_{ij}(\vec{\xi}) + \langle i0|\,\varphi-\tfrac{1}{2}(V^I_{i0}+V^I_{j\vec{\xi}})\,|j\vec{\xi}\rangle, \qquad \text{(A3)}$$

where E_i is the free-ion energy of the ith state and $\Delta_{ij}(\vec{\xi})$ is the overlap of the ith and jth functions separated by a distance $\vec{\xi}$. Since the potential contributions will nearly cancel in the core regions (for $\vec{\xi}=0$), where the small components of the relativistic spinors may be important, these components may be neglected. Also, the major contribution to matrix elements between functions on different sites comes from the interstitial regions, that is, away from the core regions where the small components may be important. Thus, the matrix elements can be calculated nonrelativistically (i.e., ignoring the small-components spinors).

The last term of (A3) contains some three-centered integrals which were essentially approximated by expanding the crystal potential in spherical harmonics and neglecting $l=4$ and higher terms (i.e., the s component of the crystal field was used since the $l=1, 2, 3$ terms are zero by symmetry). The expansion was performed about 0 and $\vec{\xi}$ and averaged to maintain a Hermitian matrix as well as to do away with the arbitrariness of the choice of origin. The errors inherent in these approximations were estimated and found to be substantially smaller than the uncertainties introduced by the exchange potential (i.e., the problem of how to include correlation).

---

†Work supported by the Materials Research Center, University of North Carolina, under Contract No. DAHC 15-67-C-0223 with the Advanced Research Projects Agency.

*Based on a thesis submitted by one of the authors (J. O.) in partial fulfillment of the requirements for the Ph. D. degree at the University of North Carolina at Chapel Hill.

[1]H. Overhof and J. Treusch, Solid State Commun. 9, 53 (1971); M. Inoue and M. Okazaki, J. Phys. Soc. Japan 31, 1315 (1971).

[2]G. E. Morse and A. W. Lawson, J. Phys. Chem. Solids 28, 939 (1967).

[3]R. Z. Bachrach and F. C. Brown, Phys. Rev. B 1, 818 (1970).

[4]D. C. Hinson and J. R. Stevenson, Phys. Rev. 159, 711 (1967).

[5]S. Tutihasi, J. Phys. Chem. Solids 12, 344 (1960); I. Lefkowitz, R. P. Lowndes, and A. D. Yoffe, J. Phys. Chem. Solids 26, 1171 (1965); W. Martienssen, *ibid.* 8, 244 (1959); H. Zinngrebe, Z. Physik 154, 495 (1959).

[6]A. D. Brothers and D. W. Lynch, Phys. Rev. 180, 911 (1969).

[7]A. J. Grant, W. Y. Liang, and A. D. Yoffe, Phil. Mag. 22, 1129 (1970).

[8]R. S. Knox, *Theory of Excitons* (Academic, New York, 1963).

[9]J. M. Hodby, J. A. Borders, F. C. Brown, and S. Foner, Phys. Rev. Letters 19, 952 (1967); H. Tamura, T. Masumi, and K. Kobayashi, J. Phys. Soc. Japan 23, 1173 (1967).

[10]Y. Makita, K. Kobayashi, M. Kanada, and T. Kawai, J. Phys. Soc. Japan 25, 816 (1968).

[11]J. W. Hodby, G. T. Jenkin, K. Kobayashi, and H. Tamura (unpublished).

[12]L. P. Howland, Phys. Rev. 109, 1927 (1958).

[13]F. Bassani, R. S. Knox, and W. B. Fowler, Phys. Rev. 137, A1217 (1965).

[14]P. M. Scop, Phys. Rev. 139, A934 (1965).

[15]Tl^+ and Br^- wave functions and potentials calculated

as in the following reference were made available to us by those authors by courtesy of the Oak Ridge National Laboratories. The Tl^{+*} states were calculated in a configuration which is the ground state with a $6s_{1/2}$ electron replaced by the state noted and the calculation carried to a new self-consistency. T. C. Tucker, L. D. Roberts, C. W. Nestor, Jr., T. A. Carlson, and F. B. Malik, Phys. Rev. 178, 998 (1969).

[16]J. E. Robinson, F. Bassani, R. S. Knox, and J. R. Schrieffer, Phys. Rev. Letters 9, 215 (1962).

[17]The validity of the LCAO method depends a great deal on the smallness of the overlap of neighboring wave functions. In this work the largest value of overlap, 0.077, is for the Tl^{+} $6s_{1/2}$-Br^{-} $4p_{3/2}$ nearest-neighbor wave functions (only considering valence basis). Maximum values reported for the LCAO calculations of KCl and AgCl are 0.07 (Ref. 12) and 0.078 (Ref. 13), respectively. The remaining smaller overlaps (including second nearest neighbors) of this work are also comparable to smaller values reported in Refs. 12 and 13.

PHYSICAL REVIEW B VOLUME 7, NUMBER 2 15 JANUARY 1973

g and Hyperfine Components of V_K Centers*

Dirk Schoemaker†
Argonne National Laboratory, Argonne, Illinois 60439
(Received 28 August 1972)

Experimental values of the g and hyperfine components of X_2^- V_K centers and Y_2^- V_K-type centers (X, Y = F, Cl, Br, I) in a large number of pure (AX) and doped ($AX:Y^-$) alkali halides have been determined through a careful analysis of their electron-paramagnetic-resonance (EPR) spectra. Expressions for the g components have been derived. For an accurate quantitative analysis, it is necessary to take into account the overlap terms in the calculation of δ, the matrix element of the orbital angular momentum $\tilde{l}$ between the $^2\Sigma_u^+$ ground state and the $^2\Pi_u$ state. A calculation for Cl_2^- yields $\delta = 0.78$. Representative experimental values for Cl_2^- and Br_2^- are $\delta = 0.73$ and 0.70, respectively. The $^2\Sigma_u^+ - {}^2\Pi_u$ energy differences thus determined decrease going from the Rb salt to the Li salt. This behavior, in general, parallels that of the $^2\Sigma_u^+ - {}^2\Sigma_g^+$ and $^2\Sigma_u^+ - {}^2\Pi_g$ energy differences which are known from the optical-absorption measurements. The crystal field splitting of the $^2\Pi_u$ state is determined from the orthorhombic character of the g tensor. Expressions for the hyperfine components have been derived which include the first- and second-order correction terms originating from the combined effect of the spin-orbit and hyperfine operators. From the analysis of the combined behavior of the orthorhombic character of the g and hyperfine (hf) components, it can be concluded that $A_\parallel > 0$ and $A_\perp > 0$ for Cl_2^-, Br_2^-, and I_2^-, and $A_\parallel > 0$ and $A_\perp < 0$ for F_2^-. The analysis of the hf components then shows that the isotropic part of the hf interaction decreases monotonically going from the Rb to the Li salt, while the anisotropic part remains approximately constant. EPR results for V_{KA}, V_{KAA}, and V_F centers are also given and they are compared with the V_K-center data.

I. INTRODUCTION

The V_K center is the fundamental trapped-hole center in the alkali halides. Its geometric structure has been well established by electron-spin-resonance,[1] optical-absorption,[2,3] and electron-nuclear-double-resonance (ENDOR) measurements.[4] The hole is self-trapped by two neighboring substitutional X^- halogen ions as a ⟨110⟩-oriented X_2^- molecule ion occupying two negative-ion sites.[5]

The understanding of the properties of the V_K center is of fundamental importance. A large number of homonuclear and heteronuclear hole centers in the alkali halides (and other materials) are either derived from it or related to it[5] (e.g., the V_{KA} centers,[6,7] the V_F centers,[7-9] and the heteronuclear V_K-type hole centers[9,10]). Furthermore, the interstitial halogen-atom centers (i.e., the H center[11,12] and the centers derived from it[13-17]) are also X_2^- molecule ions but occupying only a single negative-ion site. Finally, the excitonic luminescence in alkali halides is described in terms of a relaxed (V_K + electron) system.[5,18,19]

The properties of the V_K center, especially those of the ground state, appear to be very close to those of the $^2\Sigma_u^+$ ground state of the free X_2^- halogen molecule ion. One expects that the differences between V_K and free X_2^- will become more pronounced in the excited states, because the lattice will affect V_K-center excited states more than the ground state and will tend to delocalize them. However, no direct comparison between V_K and free X_2^- is possible for the moment, because no relevant experimental spectroscopic data are available for the latter. At present the only source for comparison can be found in the elaborate self-consistent-field–molecular-orbital (SCF–MO) calculations of Gilbert and Wahl[20] on F_2^- and Cl_2^-. These wave functions were used by Jette, Gilbert, and Das[21] in their the-